Visco-plasticity of polycrystalline tantalum - rational phenomenology in constitutive modeling

J. R. KLEPACZKO

Metz University,
Laboratory of Physics and Mechanics of Materials,
Ile du Saulcy, 57045 Metz, France,
e-mail: klepaczko@lpmm.univ-metz.fr

Dedicated to Professor Piotr Perzyna
on the occasion of his 70th birthday

CONSTITUTIVE MODELING based on the so-called rational phenomenology (materials science approach) has been applied to take into account strain hardening, strain-rate sensitivity, thermal effects and evolution of microstructure in a polycrystalline tantalum. A wide range of strain rate in shear (10^{-4} 1/s $< \dot{\Gamma} < 5*10^3$ 1/s) and homologous temperature ($0.05 < \Theta < 0.2$) is considered. Behavior of tantalum is understood as an example for BCC polycrystalline metals. The constitutive modeling provided a possibility to determine all material constants via the experimental results obtained on thin tubular specimens using a fast hydraulic machine and a torsion Hopkinson bar. Finally, the model predictions are demonstrated by numerical simulations for different history paths in strain rate and temperature.

1. Introduction

POLYCRYSTALLINE TANTALUM, symbol Ta, BBC crystalline structure, melting point $T_m = 3290$ K, density $\rho = 15.0$ [g/cm^3], and heat capacity at 25° C : $C_p = 0.140$ [J/g K], is used in many industries and not only in military applications. Its very high plasticity is very attractive in many applications, for example in cumulative charges.

Application of tantalum in extreme conditions demands extensive numerical calculations with relatively good precision. Unfortunately, practically in all cases very simple constitutive relations are used for such a purpose with pure phenomenological parameters. It is clear that more advanced approaches must be introduced in order to improve numerical calculations. Because of more efficient numerical codes and much faster computers which have been introduced recently, more advanced constitutive modeling can be used in those codes. For example, the so-called MTS model (Mechanical Threshold Stress), [1], has more recently been applied to tantalum and tantalum-tungsten alloys [2]. Still more

advanced constitutive modeling has been proposed in the series of papers by this author, [3-7]. All constitutive relations derived on the basis of materials science are founded on the concept of thermal activation processes, for example [8-11].

It is well established that plastic deformation of crystalline materials is accomplished by motion of dislocations. Dislocations are generated, multiplied, and partly annihilated during plastic deformation occurring with a specified strain rate. Velocities of edge and screw dislocations substantially increase, sometimes by several orders of magnitude, when the effective shear stress is increased above the threshold level, for example [13]. Thermal motion of atoms is manifested by temperature. The thermal vibrations with Debye frequency $\nu_D \approx 10^{13}$ $1/s$, and the vibration energy $W = kT$, where k is the Boltzmann constant and T is the absolute temperature, assist in most of the dislocation processes and cause certain rate and temperature effects in plasticity. Some processes are athermal, that is the energy of thermal vibration is not high enough to activate a process. For example, the thermal vibrations of atoms cannot play any role in generation of the dislocations by the Frank-Read multiplication mechanism, since the threshold energy is much higher than that could be supplied by the thermal vibrations, [14]. On the contrary, the movement of dislocations can be thermally activated with the assistance of the effective shear stress τ^* acting on the glide plane, [10]. In the simplest case the fundamental relation has been established between the shear strain Γ, shear strain rate $\dot{\Gamma}$ on the glide plane, the absolute temperature T and the effective shear stress τ^*, in the form of Arrhenius relation

$$(1.1) \qquad \dot{\Gamma} = \dot{\Gamma}_0 \, \exp\left[\exp(-\frac{\Delta G(\tau*)}{kT}) \right]$$

where $\dot{\Gamma}_0$ is the frequency factor related to the characteristic frequency of vibration of the moving dislocation and to the Debye frequency, $\Delta G(\tau^*)$ is the energy activation or free Gibbs energy, [8-12]. The relation in the form of the effective stress versus absolute temperature provides fundamental information on the nature of a thermally activated process of plastic deformation. If the expression for the energy of activation is linearized with respect of the effective stress, that is

$$(1.2) \qquad \Delta G = G_0 - (\tau - \tau_\mu) v* \qquad \text{where} \quad \tau* = \tau - \tau_\mu,$$

the total shear stress τ on the slip plane can be written as

$$(1.3) \qquad \tau = \tau_\mu + \frac{G_0}{v*}\left[1 - \frac{kT}{G_0} \ln\left(\frac{\dot{\Gamma}_0}{\dot{\Gamma}} \right) \right].$$

The stress component τ_μ is called the athermal stress or the internal stress. The activation volume v^* can be defined in general as

$$(1.4) \qquad v* = -\frac{\partial \Delta G}{\partial \tau*}.$$

In the case of linearization, the activation volume is determined with respect to the total stress τ

$$(1.5) \qquad v = -\frac{\partial \Delta G}{\partial \tau} \qquad \text{and} \quad v = v^*.$$

Relation $((5.4)_3)$ can be rewritten in the following form:

$$(1.6) \qquad \tau = \tau_\mu + \tau_0^* \left[1 - \frac{MkT}{G_0} \log \left(\frac{\dot{\Gamma}_0}{\dot{\Gamma}} \right) \right]$$

where M = 2.3026 (conversion factor to decimal logarithm) and $\tau_0^* = G_0/v^*$ is the threshold shear stress at $T = 0$ or $\dot{\Gamma} = \dot{\Gamma}_0$. Since the thermally activated component of the shear stress must be always positive, the following condition must be imposed on Eq. (1.6):

$$(1.7) \qquad \frac{MkT_C}{G_0} \log(\frac{\dot{\Gamma}_0}{\dot{\Gamma}_C}) \geq 1 \quad \text{or} \quad T_C \log(\frac{\dot{\Gamma}_0}{\dot{\Gamma}_C}) \geq \frac{G_0}{Mk}.$$

Values of the critical absolute temperature T_C and critical strain rate $\dot{\Gamma}_C$ define the critical point on the $(T, \dot{\Gamma})$ plane. If $T > T_C$ or $\dot{\Gamma} < \dot{\Gamma}_C$ then $\tau = \tau_\mu$.

In reality, the linear case may by a good approximation at relatively low temperatures. For example in Fig. 1 is shown the change in flow stress of a single crystal of tantalum with temperature at the strain rate $8*10^{-5}$ 1/s, the data reconstituted after [15] for three levels of shear strain: 0.01, 0.04 and 0.08. It is interesting to note, as it was stated in [15], that the changes of the flow stress with temperature are independent of the crystal orientation. Such behavior can be explained by the existence of a single thermally activated process true for all orientations. It is well known that for BCC metals the adequate process is the kinetics of the dislocation movement over the Peierls potential, [8.12]. In BCC metals the Peierls potential is relatively high, this is the potential of the lattice itself. Figure 1 shows also that the strain hardening, not taken into account in the analysis given above, must be considered in more advanced versions of constitutive modeling. The simplest approach is to include all strain hardening effects into the internal stress τ_μ. This concept leads to a variety of models proposed by different authors. The set of such models can be written as

$$(1.8) \qquad \tau = \tau(\Gamma_p, T) + \tau_0^* [1 - \frac{MkT}{G_0} \log(\frac{\dot{\Gamma}_0}{\dot{\Gamma}_p})]$$

where Γ_p is the plastic shear strain.

Even if the strain hardening effects on the flow stress are included as it is done in Eq. (1.8), this simple approach is not capable of accounting for variety of effects related to micro-structural evolution at different strain rates and

temperatures, for example [3, 16, 17]. Those effects had been studied for many decades and they have provided many data which should be included into more advanced constitutive modeling. One of such approaches is presented in the next part of this paper.
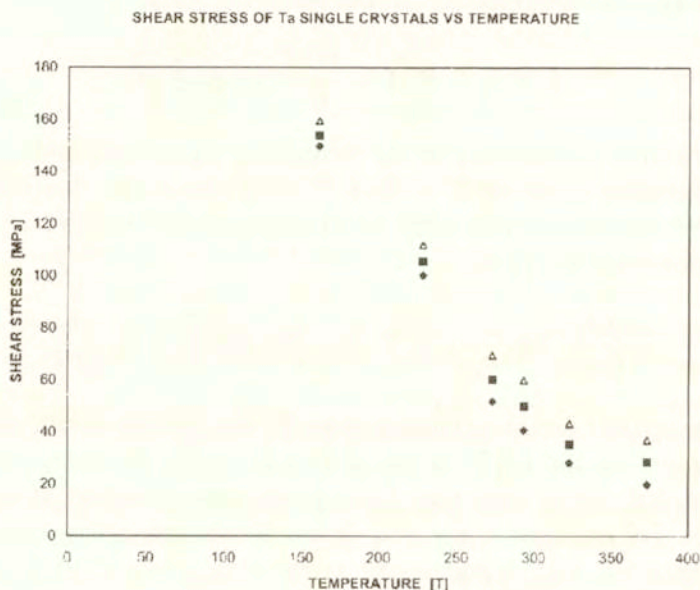
SHEAR STRESS OF Ta SINGLE CRYSTALS VS TEMPERATURE

FIG. 1. Changes in flow stress of single crystals of Ta with temperature at $\dot{\Gamma} = 8 * 10^{-5}$ 1/s, reanalyzed data after [15].

2. The constitutive formalism

The constitutive modeling applied to polycrystalline tantalum is based on a consistent approach to the kinetics of macroscopic plastic flow of metals with BCC and FCC structures. The approach is called "the rational phenomenology", [18]. All variables and parameters are defined as physically based. However, the microscopic variables are used in the macroscopic scale as the mean ones, for example density of dislocations, with no statistical specification how the transition into the mean values was obtained. It is believed that such an approach is justified for statistics of large numbers. The set of relations between particular variables and parameters combined in a specific order is called the constitutive formalism. Although in general the same or similar standard relations known in materials science are applied, their combination and use decide about efficiency and logic of the formalism.

In the approach presented here the constitutive formalism is applied with the *one* constitutive variable that is the total dislocation density ρ. It is assumed that plastic deformation in shear is the fundamental mode in metals plasticity. It is assumed further that at constant microstructure the flow stress τ consists of two components: the internal stress τ_μ and the effective stress τ^*, thus

$$(2.1) \qquad \tau = \tau_\mu[s_i, h(\dot{\Gamma}_p, T)]_{STR} + \tau^*[(s_i, \dot{\Gamma}_p, T)]_{STR}$$

where s_i is a number, so far unspecified, of internal state variables which define the current microstructure, [5,6], $h(\dot{\Gamma}_p, T)$ is the thermal-mechanical history of plastic deformation, Γ_p and $\dot{\Gamma}_p$ are, respectively, plastic shear strain and plastic shear strain rate. In the next part of the paper the subscript "p" will be omitted. It is important to note that the plastic strain does not enter directly into relation (2.9). Plastic strain can not be assumed in the materials science approach as an independent variable, or argument in constitutive relations, since the process of defect accumulation (plastic strain) depends on the past thermal-mechanical history. In relation (2.1) the internal stress τ_μ is caused, therefore, by the long-range, strong obstacles to dislocation motion, and the effective stress τ^* is due to thermally activated short-range obstacles. In fact, the internal stress τ_μ must be indirectly rate- and temperature-dependent via dislocation rearrangement and annihilation (recovery), during the whole process of plastic deformation.

In the case of *one* internal state variable assumed here as the total dislocation density ρ, Eq. (2.1) can be simplified to the form

$$(2.2) \qquad \tau = \tau_\mu[\rho, h(\dot{\Gamma}, T)] + \tau^*(\rho_m, \dot{\Gamma}, T)$$

where ρ_m is the mobile dislocation density. In the one-variable approach the mobile dislocation density is directly related to the total density by the relation

$$(2.3) \qquad \rho_m = f\rho, \quad f \le 1.$$

In general, the microstructure can be characterized by five instantaneous quantities: ρ, ρ_m, d, D and Δ, where ρ and ρ_m are the mean values over few subgrains, d, D and Δ are respectively, the subgrain diameter, the grain diameter and the mean distance between the twins, [5,6]. The explicit form for the internal stress τ_μ can be written for a constant temperature as follows, [5,6]

$$(2.4) \qquad \tau_\mu = \alpha_1 \mu b \sqrt{\rho} + \alpha_2 \mu \left(\frac{b}{d(\rho)}\right)^\delta + \alpha_3 \mu \left(\frac{b}{D}\right) + \alpha_4 \mu \left(\frac{b}{\Delta}\right).$$

The first three terms in Eq. (2.4) are related respectively to dislocation-long range obstacle interaction, evolution of sub-grain size d and the effect of grain diameter D, so-called the Hall-Petch term. The fourth term accounts for twin

formation typically observed at very low temperatures or at very high strain rates. The constants α_1, α_2, α_3, and α_4 are the interaction constants showing the fraction contribution of each micro-mechanism to the total value of the internal stress τ_μ, b is the modulus of the Burgers vector . The power δ in the second term has a dual nature, $\delta = 1.0$ for cells and small sub-grains with large mis-orientations, and $\delta = 1/2$ for "ideal" sub-grains in thermally recovered metals, [19]. Finally, μ is the shear modulus. Although evolution of sub-grains and twins are observed in BCC metals, their contribution is assumed here as the second order effect. The effect of grain diameter D is automatically included into the generalized interaction coefficient α. Equation (2.4) can be rewritten in the following form:

$$(2.5) \quad \tau_\mu = \mu\, b\, \sqrt{\rho}\left\{\alpha_1 + \alpha_2[b\,\rho\,d(\rho)]^{-1/2} + \alpha_3\,[b\,\rho\,D]^{-1/2} + \alpha_4\,[b\,\rho\,\Delta]^{-1/2}\right\}$$

The expression in the large brackets of Eq. (2.5) can be understood as a generalized coefficient $\alpha(\rho, d, D, \Delta)$ of interaction between dislocations and *all* long-range obstacles used frequently in analyses of the experimental data. With this simplification, the final form for the internal stress τ_μ and for a constant temperature case applied in this modeling, can be written as follows:

$$(2.6) \qquad\qquad \tau_\mu = \alpha_0\, \mu(T)\, b\, \sqrt{\rho[h(\dot{\Gamma}, T)]},$$

where α_0 is the interaction constant at T = 0. The dislocation-obstacle interaction must be modified to include temperature-dependent changes of elastic constants. One possibility is a simple empirical relation

$$(2.7) \qquad\qquad \mu(T) = \mu_0\,(1 - At - BT^2)$$

where A and B are the constants, with condition $\mu(T_m) = 0$, where T_m is the melting temperature. Due to the thermal softening of the lattice, the interaction constant is also temperature-dependent

$$(2.8) \qquad\qquad \alpha(T) = \alpha_0\, \frac{\mu(T)}{\mu_0}.$$

All equations outlined above constitute the fundamental framework for the first part of the constitutive formalism. The most important problem arises now, how to model the micro-structural evolution at different strain rates and temperatures.

3. Kinetics of micro-structural evolution, the internal stress

It is well established that during plastic deformation of metals at different strain rates and temperatures, the rate of strain hardening may vary substan-

tially. If the strain rate and temperature is changed during the process of deformation, such variations are the source of strain rate and temperature history effects, [3, 16, 17]. One possibility is to introduce micro-structural evolution in the modeling by a set of ordinary differential equations of the first order. Each equation describes evolution of an internal state variable as a function of plastic strain. In a general case of such modeling five differential equations should be introduced for five internal state variables, ρ_i, ρ_m, d, D, Δ, where the total dislocation density ρ is split into the immobile density ρ_i and the mobile density ρ_m

$$(3.1) \qquad \rho = \rho_i + \rho_m.$$

Since in BCC metals the evolution of the mobile dislocation density is very important, both densities must be accounted for. Some propositions and discussions of the evolution equations can be found elsewhere, [3-7]. A general notion is adopted that the evolution of microstructure can be described by the accumulation kinetics of defects, in the present case- of dislocations. Of course, the process of accumulation depends on the strain rate and temperature. It is assumed that the general form of evolution equation is given by

$$(3.2) \qquad \frac{d\rho}{d\Gamma} = M_{eff}(\rho, \dot{\Gamma}, T),$$

where M_{eff} is the effective multiplication rate of dislocations, [20]. A simple equation for structural evolution has been derived in the following form, [5],

$$(3.3) \qquad \frac{d\rho}{d\Gamma} = M_{II}(\dot{\Gamma}) - k_a(\dot{\Gamma}, T)(\rho - \rho_0)$$

where M_{II} is the multiplication factor at small plastic strains and $k_a(\dot{\Gamma}, T)$ is the rate and temperature- dependent annihilation factor, ρ_0 is the initial dislocation density. For BCC metals the multiplication factor M_{II} can be assumed as a constant at not very high strain rates and up to the temperature where annihilation micro-mechanisms (recovery) start to be intensified. The explicit mathematical form for k_a has been proposed for FCC metals in [5] and adapted for BCC structures in [21] as follows:

$$(3.4) \qquad k_a(\dot{\Gamma}, T) = k_0 \left(\frac{\dot{\Gamma}}{\dot{\Gamma}_0} \right)^{-2m_0(\dot{\Gamma}, T_a)}$$

where k_0 and m_0 are the annihilation constants at $T = 0$, m_0 is the absolute rate sensitivity of strain hardening, $\dot{\Gamma}_0$ and T_a are respectively the frequency factor and the transition temperature. If $T \leq T_a$ or $\dot{\Gamma} \geq \dot{\Gamma}_0$ then $k_a = k_0$.

When temperature and strain rate are constant, the evolution Eq. (3.3) can be integrated with the initial conditions $\rho = \rho_0$ at $\Gamma = 0$ and solution for ρ can be found in the closed form

$$(3.5) \qquad \rho(\dot{\Gamma}, T) = \rho_0 + \frac{M_{II}}{k_a[h(\dot{\Gamma}, T)]}[1 - \exp(-k_a[h(\dot{\Gamma}, T)])].$$

If the temperature is lower than T_a, Eq. (3.5) reduces to the simpler form with $k_a = k_0$ and then the explicit form for the internal stress τ_μ is

$$(3.6) \qquad \tau_\mu = \alpha(T)\,\mu_0\,b\left[\rho_0 + \frac{M_{II}}{k_0}[1 - \exp(-k_0\,\Gamma)]\right]^{1/2}, \qquad T \leq T_a.$$

It may be noted that Eq. (3.6) predicts a saturation of the internal stress at large strains. The internal stress at saturation is

$$(3.7) \qquad \tau_\mu(\Gamma \to \infty) = \alpha_0\,\mu(T)\,b\left[\rho_0 + \frac{M_{II}}{k_a(\dot{\Gamma}, T)}\right]^{1/2}, \qquad T \geq T_a.$$

$$(3.8) \qquad \tau_\mu(\Gamma \to \infty) = \alpha_0\,\mu(T)\,b\left[\rho_0 + \frac{M_{II}}{k_0}\right]^{1/2}, \qquad T \leq T_a.$$

A more exact evolution relation suitable for larger strains can be written as follows:

$$(3.9) \qquad \frac{d\rho}{d\Gamma} = M_{II}(\Gamma) + \left[k_a(\dot{\Gamma}, T)(\rho - \rho_0)\right]^{1/2} - k_a(\dot{\Gamma}, T)(\rho - \rho_0).$$

Although differential Eq. (3.8) can be integrated for constant strain rate and temperature, the inversion to find the dislocation density $\rho(\Gamma)$ is only numerically possible.

In conclusion, the approximation (3.6) assumes the absence of the rate sensitivity of strain hardening, [22], at temperatures lower than T_a. At temperatures higher than T_a the rate sensitivity of strain hardening is present and intensifies as the strain rate decreases. It may be noted that the internal stress τ_μ is temperature-dependent even at $T < T_a$ due to the temperature-dependence of the interaction constant α via temperature-dependence of the elastic constants. It has been shown previously that the approximation of the internal stress is sufficiently exact for BCC micro-structures, for example mild steels, [4, 5, 6].

4. Kinetics of micro-structural evolution, the effective stress

The effective stress τ^*, directly related to the instantaneous rate sensitivity, [22], can be determined by inversion of the generalized Arrhenius relation, [3],

$$(4.1) \qquad \dot{\Gamma} = \nu_k(\rho_m, T) \, \exp\left[-\frac{\Delta G(\tau^*, T, \rho_m)}{kT}\right]$$

where ν_k is the frequency factor and ΔG_k is the free energy of activation, k is the Boltzmann constant. It has been shown, for example in [8, 9, 12], that dislocations in BCC structures move by the thermally activated formation and propagation of kink pairs over the Peierls potential. A universal relation between ΔG_k and τ^* has been proposed in [12] in the form

$$(4.2) \qquad \Delta G_k = 2H_k(T)\left[1 - \left(\frac{\tau^*}{\tau_p^*(T)}\right)^p\right]^q,$$

where p and q are constants that characterize the shape of a thermally activated obstacle, and in this case the Peierls potential, $2H_k$ is the total activation energy necessary to form a double kink and overcome the potential, $\tau_p * (T)$ is the Peierls stress. Both constants are temperature-dependent through the temperature changes of the elastic shear modulus, thus

$$(4.3) \qquad 2H_k(T) = 2H_k^0\frac{\mu(T)}{\mu_0} \quad \text{and} \quad \tau_p^*(T) = \tau_p^0\frac{\mu(T)}{\mu_0},$$

where H_k^0, τ_p^0, and μ_0 are respectively the activation energy, Peierls stress, and shear modulus, all in 0 K.

When the dislocation kinetics is controlled by thermally activated overcoming of obstacle, one obtains the pre-exponential factor in the following form, [11],

$$(4.4) \qquad \nu(\rho_m, T) = \rho_m \frac{bA(T)}{L(T)}\left(\frac{b}{2l(T)}\nu_D\right)$$

l is the length of the dislocation segment involved in the thermal activation, A is the area swept out by the mobile dislocation following the successful attempt, ν_D is the vibration frequency of the lattice (Debye frequency). Therefore ρ_m indicates the number of places where the thermal activation occurs, $\nu_i = (b/2L(T))\nu_D$, ν_i is the vibration frequency of the pinned dislocation of length L involved in the event, $l < L$. For the case of double kink, the pre-exponential factor can be written as

$$(4.5) \qquad \nu_k = n\,\rho_m\,b^2\,\nu_D \quad \text{and} \quad n = \frac{aL}{2\,l_c^2},$$

l_c is the critical length of the kink segment of dislocation. Assuming that $A = La$ and $a = b$, n becomes the non-dimensional coefficient characterizing the geometry of the double kink formation, [4]. In general, the dislocation length L is much greater than the dislocation segment l involved in the thermal activation.

The second internal state variable that enters the pre-exponential factor is the mobile dislocation density ρ_m. Since even in relatively pure BCC metals the stationary dislocations are pinned, for example by Cottrell atmospheres, [23], evolution of the mobile dislocation density must be accounted for. One, and the simplest, possibility is to assume $\rho_m = f\rho$, where f is the fraction of the total density, $f < 1$; f may change as a function of ρ and temperature. Although it can be shown that the constant value of f gives satisfactory quantitative results, more exact analyses of experimental data, mostly for steels, indicate that the fraction f is a more complicated function of ρ, $\dot{\Gamma}$ and T. At relatively low homologous temperatures, and under the assumption that the evolution of the mobile dislocation density is independent of the immobile density, a differential equation introduced in [4] has the following form:

$$(4.6) \qquad \frac{d\rho_m}{d\rho} = \frac{\beta}{\rho}$$

where β is the material constant. The solution of (4.6) with the initial conditions $\rho_m = \rho_{m0}$ at $\rho = \rho_0$ has the following form:

$$(4.7) \qquad \rho_m = \rho_{m0} + \beta \ln \left(\frac{\rho}{\rho_0} \right).$$

Thus, the evolution of the mobile dislocation density is a complicated function of plastic strain since in Eq. (4.7) the solution for ρ, Eq. (3.5) or (3.6), depends on the temperature domain of deformation. Thus, the solution for ρ must be introduced into (4.7). It is interesting to mention that the limit of the mobile dislocation density ρ_m is the saturation level of the total density with $f = 1$, $\rho_m(M/k_a)$

$$(4.8) \qquad \rho_m(\frac{M_{II}}{k_a}) = \rho_{m0} + \beta \frac{k_a}{M_{II}} \ln \left(\frac{M_{II}}{\rho_0 \, k_a} \right), \qquad \rho_{m0} < \rho < M_{II}/k_a.$$

The solution for the mobile dislocation density makes it possible to determine the pre exponential factor in Eq. (4.5) and define completely the effective stress τ^*. After introduction of (4.2) and (4.5) into (4.1) and inversion, the explicit expression for τ^* is obtained

$$(4.9) \qquad \tau^*(\rho, \dot{\Gamma}, T) = \tau_p^* \left\{ 1 - \left[\frac{kT}{2H_k} \log \left(\frac{n\,\rho_m\, b^2\, \nu_D}{\dot{\Gamma}} \right) \right]^{1/q} \right\}^{1/p}.$$

The total stress is defined by Eq. (2.2). In this manner the model is complete including the following Eqs. (2.6), (2.7), (2.8), (3.1), (3.4), (3.5), (4.2), (4.3), (4.5), (4.7) and (4.9). The total number of constants is 21, including the absolute physical constants: $b, H_k, n, p, q, T_m, \mu_0, \nu_D$ and τ_p^0, total 9, which can be found theoretically from physical analyses; the rest, that is 12 constants, are the constants related directly to specific material behavior and conditions of deformation.

5. Constitutive modeling of polycrystalline tantalum

The constitutive formalism applied in the case of tantalum is similar to the simplified constitutive model applied earlier to mild steels, [4]. The rate sensitivity of strain hardening is neglected, that means that relatively low homologous temperatures are considered, and the following relations are applied: (2.6), (2.7), (2.8), (3.1), (3.6), (4.2), (4.3), (4.5) and (4.7). The constants have been identified from experiments.

Experiments reported in [24] have been performed at room temperature on thin tubular specimens of annealed polycrystalline Ta in LPMM-Metz on a fast hydraulic machine, and in CEA-DAM (the French Atomic Energy Commission) on a Split Hopkinsion Torsion Bar (SHTB). Those two experimental setups permitted to cover the shear strain rates from $3*10^{-4}$ 1/s to $3*10^2$ 1/s not only at constant imposed values but also in the changed-strain-rate mode, that is from low to high and from high to low strain rates. The strain rate changes from lower to higher and from higher to lower strain rate were applied with the loading-unloading procedure for two initial pre-strains. The final results reproduced after [24] are shown in Fig. 2 and Fig. 3. The behavior is typical for polycrystalline BCC metals. At low strain rate, $3*10^{-4}$ 1/s, relatively high strain-hardening is observed, but at $3*10^2$ 1/s the rate of strain-hardening is positive at lower strains, say up to 0.3 and then zero or even negative. It may be mentioned that at strain rates higher than ~ 50 1/s the process of plastic deformation is practically adiabatic and about 90% of plastic work is converted into heat. Since BBC metals are very sensitive to temperature, as it is shown in Fig. 1, the decrement of stress due to adiabatic heating is not negligible and in order to compare $\tau(\Gamma)$ at different strain rates, specially at lower and at higher ones, the high strain-rate curves should be converted into isothermal conditions. A more exact discussion and a simple method of conversion were given in [17]. In the present analysis the conversion is neglected because only simplified modeling is analyzed numerically. Experiments with changed strain rates confirmed for tantalum the existence of the strain rate history effects revealed earlier for soft steels, [17, 25]. A change of strain rate from low to high values produces "overshoot" of flow stress, that is the flow stress is higher at the same strain rate as that applied in a constant

strain, rate deformation. In the case of tantalum strain rate change from $3*10^{-4}$ 1/s to $3*10^2$ 1/s, Fig. 2, and from $1.5*10^{-2}$ 1/s to $3*10^2$ 1/s produces rather small overshoots. On the contrary, change of strain rate from high to low, that is from $3*10^2$ 1/s to $3*10^{-4}$ 1/s, revealed a substantial "undershoot", that is all $\tau(\Gamma)$ curves are lower than that obtained at the same constant strain rate. Those strain rate history effects are quite opposite than those observed many times in various of FCC metals, for example [3, 5, 16]. It is clear that specific strain-rate history effects are found in tantalum.
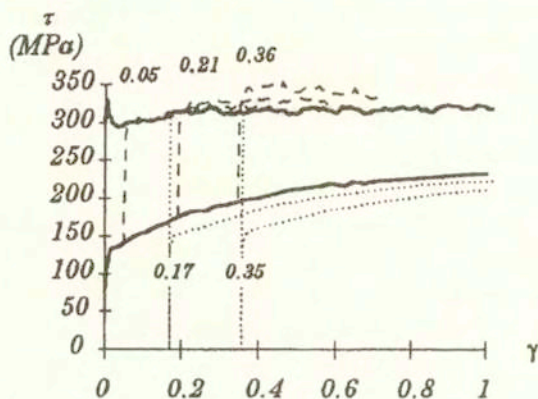

FIG. 2. Results of torsion experiments on polycrystalline Ta at two strain rates: $\dot{\Gamma} = 3.10^{-4}$ 1/s and $\dot{\Gamma} = 3*10^2$ 1/s; Constant and changed strain rates at three levels of prestrain, after [24].
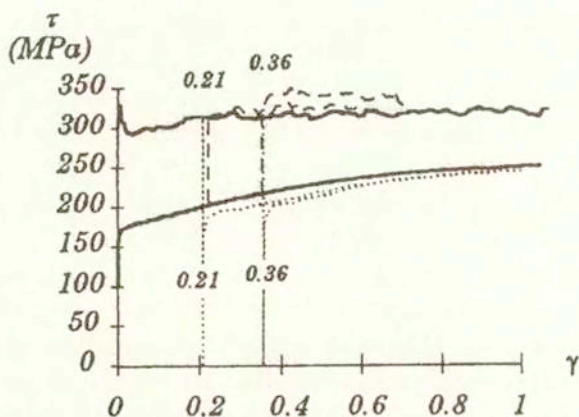

FIG. 3. Results of torsion experiments on polycrystalline Ta at two strain rates: $\dot{\Gamma} = 1.5*10^{-2}$ 1/s and $\dot{\Gamma} = 3*10^2$ 1/s; Constant and changed strain rates at two levels of prestrain, after [24].

The main task of this study was to apply a simplified version of the constitutive formalism with a possibility to model not only the behavior at constant strain rates but also the strain-rate history effects. The micro-structural evolution of the internal stress, dependent on strain-rate and temperature, has been neglected. The evolution of the internal stress is rate independent and was taken into account by relation (3.6). A complete set of relations describing the effective stress was used in numerical modeling, that is Eqs. (4.7) and (4.9).

In order to identify all material constants at $T = 300$ K it was assumed that $\tau^* \approx 0$ at strain rate 10^{-4} 1/s and the coefficient of interaction is $\alpha = 0.5$, for example [12]. The elastic shear modulus at RT is assumed as $\mu = 72$ GPa, and the Burgers vector b $= 2.86*10^{-8}$ cm. By application of the optimization procedure by the least square method the following values of the material constants have been found: $\rho_0 = 1.25*10^{10}$ 1/cm^2, $M_{II} = 9.8*10^{11}$ 1/cm^2, $k_a = 2.2$. Those values permit to calculate the internal stress at RT.
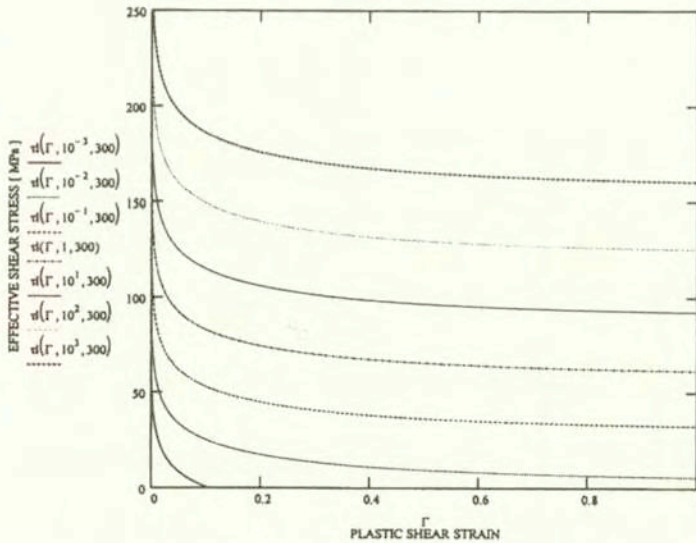

FIG. 4. Numerical calculation of the effective shear stress τ^* for Ta with plastic shear strain for 9 shear strain rates from $\dot{\Gamma} = 3 * 10^{-4}$ 1/s to $\dot{\Gamma} = 10^3$ 1/s, T=300 K.

In order to estimate the effective stress, values of the constants p and q were obtained from the literature data reporting the rate and temperature-sensitivity of Ta, [24], as $p = 1$ and $q = 8/5$, the energy of the obstacle $\Delta G_0 = 0.62$ eV. The Peierls shear stress at $T = 0$ K has been assumed as $\tau_p^* = 515$ MPa. The second set of constants allows to calculate the effective stress at RT. The effective stress τ^* at $T = 300$ K is shown as a function of shear strain in Fig. 4 for different strain
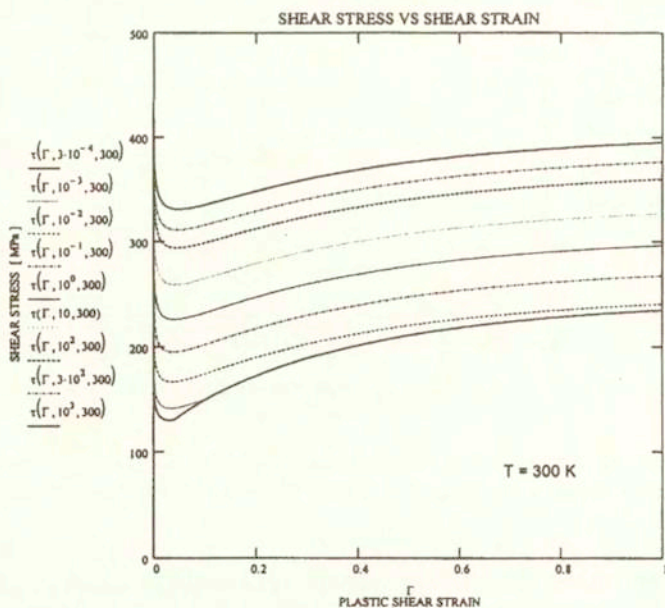
SHEAR STRESS VS SHEAR STRAIN

$\tau\left(\Gamma, 3\cdot10^{-4}, 300\right)$
$\overline{\tau\left(\Gamma, 10^{-3}, 300\right)}$
$\tau\left(\Gamma, 10^{-2}, 300\right)$
$\tau\left(\Gamma, 10^{-1}, 300\right)$
$\tau\left(\Gamma, 10^{0}, 300\right)$
$\tau(\Gamma, 10, 300)$
$\tau\left(\Gamma, 10^{2}, 300\right)$
$\tau\left(\Gamma, 3\cdot10^{2}, 300\right)$
$\overline{\tau\left(\Gamma, 10^{3}, 300\right)}$

SHEAR STRESS [MPa]

T = 300 K

PLASTIC SHEAR STRAIN

SHEAR STRESS VS SHEAR STRAIN

$\tau\left(\Gamma, 3\cdot10^{-4}, 300\right)$
$\overline{\tau\left(\Gamma, 10^{-3}, 300\right)}$
$\tau\left(\Gamma, 10^{-2}, 300\right)$
$\tau\left(\Gamma, 10^{-1}, 300\right)$
$\tau\left(\Gamma, 10^{0}, 300\right)$
$\tau(\Gamma, 10, 300)$
$\tau\left(\Gamma, 10^{2}, 300\right)$
$\tau\left(\Gamma, 3\cdot10^{2}, 300\right)$
$\tau\left(\Gamma, 10^{3}, 300\right)$
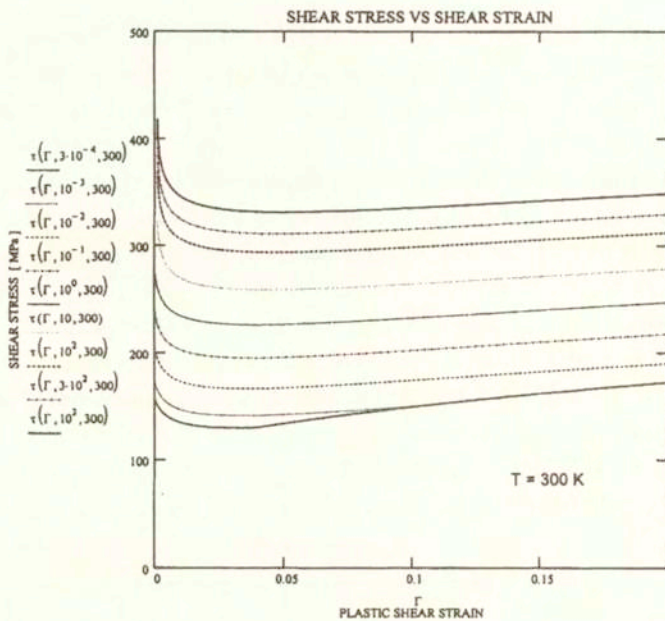
SHEAR STRESS [MPa]

T = 300 K

PLASTIC SHEAR STRAIN

FIG. 5. Numerical calculation of the flow stress τ for Ta with plastic strain for 9 shear strain rates, steps in strain rate are the same as in Fig. 4, $T = 300$ K; (a) range of strain from 0 to 0.2. (b) range of strain from 0 to 1.0.

[472]

rates from $3*10^{-4}$ 1/s to 10^3 1/s. At low strain rates the effective stress relaxes very quickly to zero at specific strain which could be obtained from the condition: $\tau^* = 0$ at $(\dot{\Gamma}_C, T_C)$. In tantalum, as in all BCC metals, the rate-sensitivity of the effective stress is very high, [25].

The result of calculations of the flow stress at different strain rates, the same as assumed for τ^* calculations, is shown in Fig. 5.

Because all curves are calculated at $T = 300$ K and the thermal softening occurring normally at higher strain rates is neglected, the curves at strain rates 10 1/s, 10^2 1/s and $3*10^2$1/s show slightly higher rate of strain hardening than in experiments.

However, the stress levels for lower strains (a less intense adiabatic heating) are almost exactly the same as a found experimentally. The upper and lower yield stress is also determined. Although the material constants have been estimated for RT, the model includes also all features of temperature-dependence at medium and low temperatures. The temperature effect on the flow stress is shown in Fig. 6 for two levels of shear strain, $\Gamma = 0$ and $\Gamma = 1.0$, and three values of strain rate: $3*10^{-4}$ 1/s, $3*10^2$ 1/s and $5*10^3$ 1/s. As expected, the critical points $(\dot{\Gamma}_C, T_C)$ at different strain rates are shifted to higher temperatures.

Another important part of the modeling is a question how to depict the strain rate history effects. An attempt reported in [26] to approximate the same experimental data was not so successful in the sense that some constants should be adjusted to the current conditions. Here a hypothesis is pursued that when the strain rate is increased, more and more mobile dislocations are generated. This assumption will lead to history-sensitive pre-exponential factor ν_k, Eq. (4.5). The differential equation for evolution of the mobile dislocation density, Eq. (4.6), does not encompass directly the strain rate. Therefore, this equation has been modified in the following way

$$(5.1) \qquad \frac{d\rho_m}{d\rho_i} = \frac{\beta}{\rho_i} + C(\dot{\Gamma}).$$

Solution with the initial conditions: $\rho_m = \rho_{m0}$ when $\rho_i = \rho_{i0}$ is in the form

$$(5.2) \qquad \rho_m(\rho_i, \Gamma, \dot{\Gamma}) = \rho_{m0} + \beta \ln\left(\frac{\rho_i(\Gamma)}{\rho_{i0}}\right) + (\rho_i(\Gamma) - \rho_{i0})C(\dot{\Gamma}).$$

Since this approach is purely empirical the explicit expression for $C(\dot{\Gamma})$ is assumed as

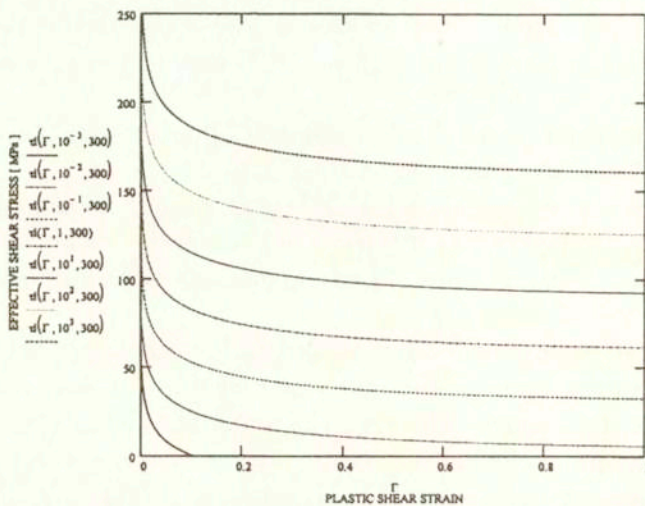$$(5.3) \qquad C(\dot{\Gamma}) = \eta \ln\left(\frac{\dot{\Gamma}}{\dot{\Gamma}_0}\right).$$

FIG. 6. Numerical calculation of the flow stress for Ta with temperature for two levels of strain and three strain rates: $\dot{\Gamma} = 3*10^{-4}$ 1/s, $3*10^2$ 1/s and $5*10^3$ 1/s.
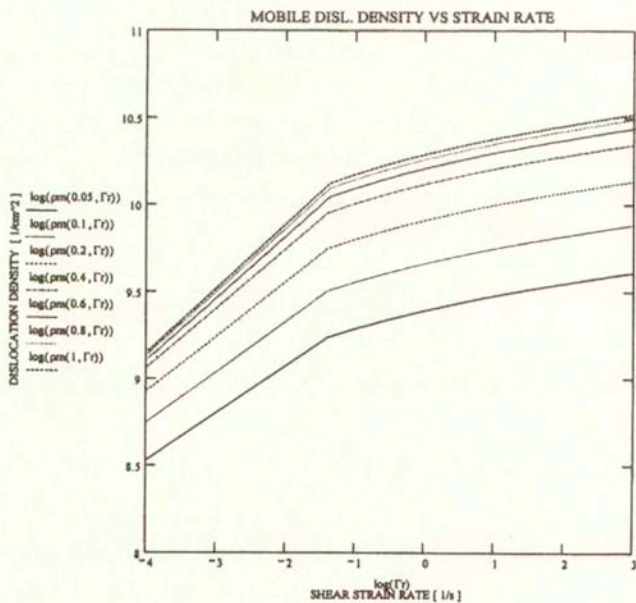

FIG. 7. Mobile dislocation density calculated after Eqs. (5.2) and (5.3) in $\log(\rho_m)$ $[1/cm^2]$ vs. $\log(\dot{\Gamma})$ [1/s] for 7 different strains from 0.05 to 1.0.
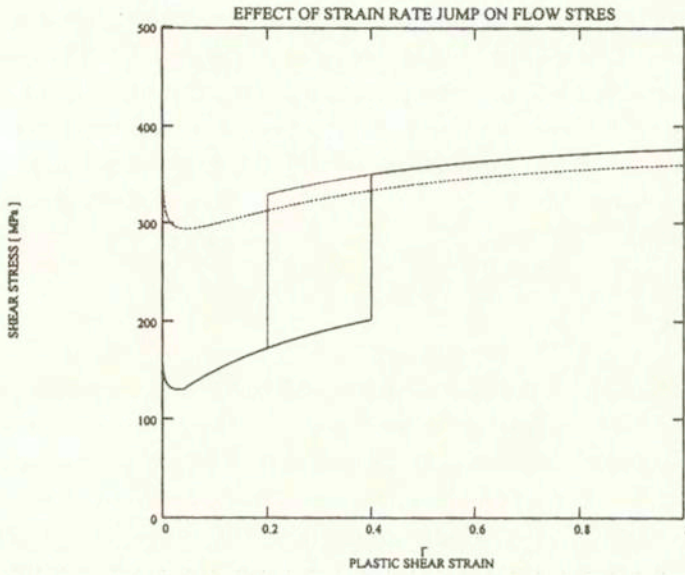
[474]

EFFECT OF STRAIN RATE JUMP ON FLOW STRES

FIG. 8. Schematic simulation of strain rate jump test from $\dot{\Gamma}$ $3*10^{-4}$ 1/s to $3*10^2$ 1/s for two prestrains Γ : 0.2 and 0.4.

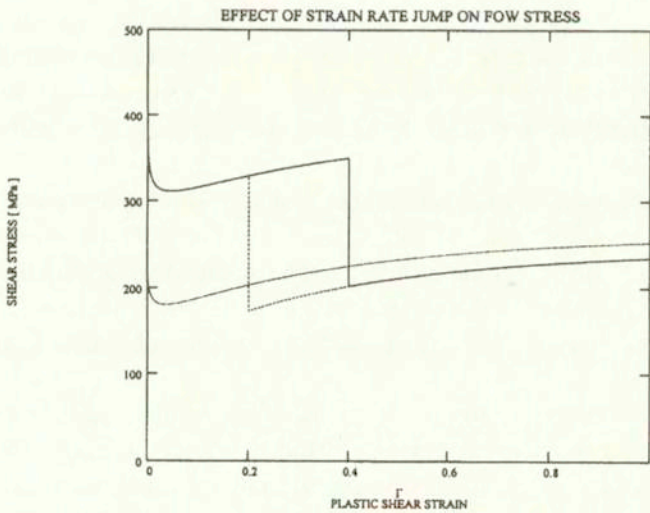EFFECT OF STRAIN RATE JUMP ON FOW STRESS

FIG. 9. Schematic simulation of strain rate jump test from $\dot{\Gamma}$ $3*10^2$1/s to $3*10^{-4}$ 1/s for two prestrains Γ : 0.2 and 0.4.

With the constants $\beta = 10^9$ cm $^{-2}$ and $\eta = 5*10^{-2}$, the evolution of the mobile dislocation density in the double logarithmic scale for different levels of

strain is shown in Fig. 7. That relation was used to calculate the strain rate jump tests from $3*10^{-4}$ 1/s to $3*10^2$ 1/s at two strains: 0.2 and 0.4. The result is shown in Fig. 8. Similar calculations were performed with the jump from $3*10^2$ 1/s to $3*10^{-4}$ 1/s, the result is shown in Fig. 9. It is clear that those artificial simulations yield results as expected, the overshoot and the undershoot are obtained. Of course, in the future a more vigorous analysis is needed from the point of view of materials science.

6. Conclusions

It has been shown that the constitutive formalism in its simplified form can approach visco-plastic behavior of polycrystalline tantalum at low as well as at relatively high strain rates. In this version of modeling, all material constants have been identified and applied in numerical analyses. As it is shown in Fig. 6, the simplified model has its limits concerning the range of temperature. The temperature limit is estimated as $T \approx 400$ K. The room temperature constitutes for tantalum the homologous temperature $\Theta_{RT} = 0.091$ and 400 K yields $\Theta = 0.122$. Thus, the modeling of visco-plasticity around room temperature is practically limited to the low temperature behavior. A complete model should include rate and temperature-dependent dislocation annihilation and rearrangement in the form of Eqs. (3.4) and (3.5). However, the simplified version can approach quantitatively the shear stress – shear strain characteristics within wide ranges of strains and strain rates. Of course, use of the formalism in 3D is possible, especially in the more advanced numerical calculations, by application of some visco-plasticity theory, for example [27, 28].

Since some applications of polycrystalline tantalum takes place frequently in the form of plates after cold rolling, a problem of anisotropy arises, for example [29,30]. In the 1D formalism presented here the isotropy is assumed, however it is important to mention that the interaction constant α in Eqs. (2.6) and (3.6) has a directional character and an anisotropy can be introduced directly in that way.

In general, constitutive formalisms based on the materials science approach should be introduced into variety of advanced numerical codes. Such modeling includes evolution of microstructure at different strain rates and temperatures, a very important factor at high strain rates.

References

1. P. S. FOLLANSBEE and U. F. KOCKS, *A constitutive description of the deformation of copper based on the use of mechanical threshold stress as an internal state variable*, Acta Metallurgica, **36**, 81, 1988.

2. S. R. CHEN and G. T.GRAY III, *Constitutive behavior of tantalum and tantalum-tungsten alloys*, Met. Trans. **27A**, 2994, 1996.

3. J. R. KLEPACZKO, *Thermally activated flow and strain rate history effects for some polycrystalline fcc metals*, Material Science and Engineering, **18**, 121, 1975.

4. J. R. KLEPACZKO, *An engineering model for yielding and plastic flow of ferritic steels*, in: High Energy Rate Fabrication, ASME, 45, New York 1984.

5. J. R. KLEPACZKO, *Modeling of structural evolution at medium and medium strain rates, FCC and BCC metals,* [in:]Constitutive Relations and Their Physical Basis, Riso Natl. Laboratory, 387, Roskilde, Denmark, 1987.

6. J. R. KLEPACZKO, *A general approach to rate sensitivity and constitutive modeling of fcc and bcc metals*, [in:] Impact: Effects of Fast Transient Loadings, A.A.Balkema, Rotterdam, Netherlands, 3, 1988.

7. J. R. KLEPACZKO, *Constitutive modeling in dynamic plasticity based on physical state variables: A review*, [in:] Int. Conf. on Mechanical and Physical Behaviour of Materials under Dynamic Loading, Les editions de physique, Les Ulis, France, C3-553, 1988.

8. J. FRIEDEL, *Les Dislocations, Gauthier-Villars,* Paris, English translation: Addison - Wesley, Reading, Massachsetts, 1964.

9. H. CONRAD, *Thermally activated deformation in metals,* Journal of Metals, **16**, 582, 1964.

10. A. SEEGER, *The mechanism of glide and work hardening in FCC and HCP metals*, in: Dislocations and Mechanical Properties of Crystals, p.271, J.Wiley, New York, 1957.

11. B. DE MEESTER, C. YIN, M. DONNER and H. CONRAD, *Thermally activated deformation in solids*, in: Rate Processes in Plastic Deformation of Materials, ASM, New York, 175, 1974.

12. U. F. KOCKS, A. S. ARGON and M. F. ASHBY, *Thermodynamics and Kinetics of Slip*, Pergamon Press, Oxford, England 1975.

13. W. G. JOHNSTON and J. J. GILMAN, *Dislocation velocities, dislocation densities, and plastic flow in lithium fluoride crystals*, Journal of Applied Physics, **31**, 632, 1959.

14. F. C. FRANK and W. T. READ, *Multiplication process for slow moving dislocations*, Physics Review, **79**, 772, 1950.

15. B. MORDIKE, *Plastic deformation of zone refined tantalum single crystals*, Zeitschrift fur Metallkunde, **53**, 586, 1962.

16. J. R. KLEPACZKO and J. DUFFY, *Strain rate and temperature memory effects for some polycrystalline FCC metals*, Proc. Conf. on Mechanical Properties of Materials at High Rates of Strain, Ser. No. 21, The Institute of Physics, Oxford, England p. 91, 1974.

17. J. R. KLEPACZKO and J. DUFFY, *Strain rate history effects in Body-Centered-Cubic metals*, in: Mechanical Testing for Deformation Model Development, ASTM STP 765, ASTM, p. 251, 1974.

18. H. J. FROST and M. F. ASHBY, *Deformation-mechanism maps: the plasticity and creep of metals and ceramics*, Pergamon Press, Oxford 1982.

19. F. R. N. NABARRO, *Work hardening in face-centered cubic single crystals*, [in:] Strength of Metals and Alloys, Proc. International Symposium CMA-7, Pergamon Press, **3**, p.545, Oxford 1986.

20. J. J. Gilman, *Micromechanics of flow of solids*, Mc Graw-Hill, New York 1969.

21. N. E. Zeghib, *Etude experimentale et modelisation de la deformation plastique tenant compte du vieillissement dynamique, cas ses aciers doux*, These de Doctorat, Universite de Metz, France, 1990.

22. J. R. Klepaczko and C. Y. Chiem, *On rate sensitivity of FCC metals, instantaneous rate sensitivity and rate sensitivity of strain hardening*, Journal of the Mechanics and Physics of Solids, **34**, 29, 1986.

23. A. H. Cottrell, *Dislocations and plastic flow in crystals*, Oxford University Press, London 1953.

24. F. Buy, *Etude experimentale et modelisation du comportement plastique d'un tanatle. Prose en compte de la vitesse de deformation et du trajet de chargement*, These de Doctorat, Universite de Metz, France, 1996.

25. J. R. Klepaczko, *The relation of thermally activated flow in BCC metals and ferritic steels to strain rate history effects*, Technical Report, Division of Engineering, Brown University, Providence, (April 1981).

26. F. Buy, J. Farre, J. R. Klepaczko and G. Talabart, *Evaluation of the parameters of constitutive model for b.c.c. metals based on thermal activation*, [in:] Proc. of Int.Conf. on Mechanical and Physical Behavior of Materials under Dynamic Loading, Coll.C3, Les editions de physique, Les Ulis, France, p. C3-631, 1997.

27. P. Perzyna, *The constitutive equations for rate-sensitive materials*, Quart. Applied Mathematics, **20**, 321, 1963.

28. S. R. Bodner, *Unified plasticity for engineering applications*, Kluwer Academic- Plenum Publishers, New York 2002.

29. S. I. Wright, G. T. Gray III and A. D. Rollet, *Textural and microstructural gradient effects on the mechanical behavior of a tantalum plate*, Met. Mat. Trans., **25A**, 1025, 1994.

30. P. J. Maudlin, J. F. Bingert, J. W. House and S. R. Chen, *On the modeling of the Taylor cylinder test for orthotropic textured materials: experiments and simulations*, Int. Journal of Plasticity, **15**, 139, 1999.